

Mapping of quantum well eigenstates with semimagnetic probes

E. Kłopotowski,¹ A. Gruszczyńska,¹ E. Janik,¹ M. Wiater,¹ P. Kossacki,² G. Karczewski,¹ and T. Wojtowicz¹

¹*Institute of Physics, Polish Academy of Sciences, al. Lotników 32/46 02-668 Warsaw, Poland*

²*Institute of Experimental Physics, Warsaw University, ul. Hoża 69 00-681 Warsaw, Poland*

(Dated: December 3, 2018)

We present results of transmission measurements on CdTe quantum wells with thin semimagnetic Cd_{1-x}Mn_xTe probe layers embedded in various positions along the growth axis. The presence of the probes allow us to map the probability density functions by two independent methods: analyzing the exciton energy position and the exciton Zeeman splitting. We apply both approaches to map the first three quantum well eigenstates and we find that both of them yield equally accurate results.

PACS numbers: 68.65.Fg 78.66.Hf 71.35.Cc 71.70.Gm

I. INTRODUCTION

The information about a quantum state is given by its energy E and its wave-function ψ . Although it is easy to measure the former, the experimental access to the latter is more difficult. In semiconductors, since the advent of epitaxial growth methods, band-gap engineering and tailoring of the eigenstates have become possible and retrieving the information inscribed in the wave-functions became necessary. The access to ψ is gained through the probability density (PD) functions $|\psi|^2$. One way of probing the PDs in quantum wells (QWs) is to introduce a highly localized potential perturbation with precisely controlled position along the growth axis. The perturbation shifts the eigenenergies of the system allowing to obtain the PD at the location of the probe in either an optical¹ or a transport² experiment. Another way is to introduce a layer containing magnetic ions, which in an external magnetic field give rise to a Zeeman effect larger than in the case of an unperturbed QW^{3,4,5}. This latter method allowed mapping of PDs in single³ or coupled multiple QWs⁵. In the first case, only the ground state PD was accessed and in the second, only relative, integrated PD values were obtained. In this work we apply both approaches to extract the PDs: we introduce magnetic probes and measure both the Zeeman effect and the shift of excitonic transitions in interband absorption. In this way, we map PD functions of the ground and the first two excited states of a CdTe QW sandwiched between Cd_{1-y}Mg_yTe barriers. As a PD probe, we use a layer of Cd_{1-x}Mn_xTe, where a part of the Cd cations are substituted with Mn²⁺ ions.

Incorporation of magnetic ions into a semiconductor matrix gives a new class of materials usually referred to as diluted magnetic semiconductors (DMS)⁶. Most commonly, the substituting atoms are transition metal ions with partially filled d -shells (Mn²⁺ ions have a half filled d -shell), which gives rise to a localized magnetic moment. Exchange interaction between localized spins of the d -shell electrons and band carriers leads to Zeeman effects enhanced by up to three orders of magnitude. To write the electronic wave-function in a DMS, we assume that the electrons adjust quasi-instantaneously to the arrange-

ment of localized spins. In this adiabatic approximation the electronic wave-function reads⁷:

$$\Psi(\vec{r}; \vec{S}_1, \dots, \vec{S}_N) = \Psi(\vec{r}; \vec{S}_i) = \psi(\vec{r}; \vec{S}_i) \Phi(\{\vec{S}_i\}) \quad (1)$$

where $\{\vec{S}_i\}$ denotes the set of all quantum numbers describing the system of magnetic ions. The $s, p - d$ exchange interaction is described by the Hamiltonian:

$$H_{sp-d} = \sum_{\vec{R}_i} J^{sp-d}(\vec{r} - \vec{R}_i) \vec{S}_i \vec{\sigma} \quad (2)$$

where \vec{r} and \vec{R}_i are the spatial and $\vec{\sigma}$ and \vec{S}_i are the spin coordinates of a band electron and a localized ion, respectively. As a consequence of the localized character of the d -shell electrons, the exchange constant is usually approximated by a collision term: $J^{sp-d}(\vec{r} - \vec{R}_i) = J^{sp-d} \delta(\vec{r} - \vec{R}_i)$.

The $s-d$ exchange interaction leads therefore to a conduction band splitting given by:

$$\Delta E_c = \sum_i \langle \Phi | S_i | \Phi \rangle N_0 \alpha |\phi_c(X_i, Y_i)|^2 |\varphi_c(Z_i)|^2 \quad (3)$$

where (X_i, Y_i, Z_i) , are the coordinates of a i th Mn ion, N_0 is the number of cation sites per unit volume, and α is the $s-d$ exchange integral. In the above, we factorized the electron wave-function into components dependent on the in-plane and perpendicular coordinates: $\psi(\vec{r}) = \phi(x, y) \varphi(z)$. Such a procedure is not always justified when interband absorption is involved as the electron-hole Coulomb interaction mixes these degrees of freedom. However, we checked that in our case this mixing is negligible and in mapping experiments it leads to errors smaller than those resulting from compositional fluctuations and temperature instability.

If the function $\varphi(z)$ does not change substantially along the thickness of the probe layer, we can substitute the summation over Z_i with a value of $\varphi(z)$ at the Mn layer location Z_{Mn} . Moreover, assuming uniform distribution of Mn ions in the QW plane we can average $\phi_c(x, y)$ over in-plane ion coordinates and obtain the electron Zeeman splitting proportional to the layer magnetization M_L ⁸:

$$\begin{aligned}\Delta E_c &= N_0\alpha|\varphi_c(Z_{Mn})|^2\overline{|\phi_c(X_i, Y_i)|^2\Sigma_i\langle\Phi|S_i|\Phi\rangle} = \\ &= N_0\alpha|\varphi_c(Z_{Mn})|^2 \cdot M_L\end{aligned}\quad (4)$$

where for $\text{Cd}_{1-x}\text{Mn}_x\text{Te}$ the conduction band exchange constant is⁹: $N_0\alpha = 0.22$ eV.

It is thus seen from Eq. 4 that electron Zeeman splitting is proportional to the PD of finding an electron in the Mn layer. However, in an interband absorption experiment we measure the excitonic Zeeman splitting, which is a sum of electron and hole splittings:

$$\Delta E_Z = (N_0\alpha \cdot |\varphi_c(Z_{Mn})|^2 - N_0\beta \cdot |\varphi_v(Z_{Mn})|^2) \cdot M_L \quad (5)$$

where $N_0\beta = -0.88$ eV is the valence band exchange constant⁹.

It can be seen from the above that measuring excitonic Zeeman splitting for a series of samples, where the Mn ions are located at various positions Z_{Mn} , allows to map a PD function *weighted* with *sp-d* exchange integrals $N_0\alpha$ and $N_0\beta$ contrary to the usual assumption^{3,5} that the heavy hole PD is mapped.

Magnetic dopants not only give rise to magneto-optical effects, but also introduce a local potential. In the first order perturbation theory, a potential of the form: $V(\delta(z - Z_{Mn}))$ located at the position Z_{Mn} shifts the electron energy E^0 of the eigenstate $\varphi_c(z)$ by:

$$E'_c - E_c^0 = V|\varphi_c(Z_{Mn})|^2 \quad (6)$$

where V is the perturbing potential, given by the chemical shift of the respective bands. Therefore, for electrons and holes the shift is proportional to conduction and valence band offset, respectively. As a result, the shift of the excitonic transition reads:

$$\Delta E_S = E'_X - E_X^0 = \varrho_c V|\varphi_c(Z_{Mn})|^2 + \varrho_v V|\varphi_v(Z_{Mn})|^2 \quad (7)$$

where ϱ_c and ϱ_v are conduction and valence band offsets, respectively and E_X^0 is the energy of the unperturbed state. Therefore, measuring the shift of the exciton energy, we can map a PD function weighted with band offsets. In the following, we took a valence band offset $\varrho_v = 0.4$ ^{10,11} and assumed a linear dependence of the chemical shift on the Mn composition⁶: $V = 1592$ meV $\cdot x_{Mn}$.

II. SAMPLES AND EXPERIMENT

Designing samples for mapping experiments using semimagnetic probes one has to bear in mind that the profiles of $\text{CdTe}/\text{Cd}_{1-x}\text{Mn}_x\text{Te}$ interfaces are broadened along the growth axis due to complete exchange of Cd and Mn ions during growth and thus absence of segregation processes¹². Consequently, although we aim to

obtain thin probe layers, the probe ions are always distributed among a couple of adjacent monolayers with the composition profile peaked at Z_{Mn} . Moreover, we have to take into account the antiferromagnetic coupling between Mn ions, which decreases substantially the magnetization and as a result also the splitting, as seen in Eq. 5. Therefore, the composition of the probe layers has to be low enough to assure a small number of nearest neighbor Mn pairs to avoid the antiferromagnetic coupling.

The samples were grown on (001) oriented GaAs substrates by molecular beam epitaxy. Substrate temperature was 230°C, which assures a high sample quality and relatively low interface broadening¹². 3.5 μm $\text{Cd}_{1-y}\text{Mg}_y\text{Te}$ buffer was deposited before the growth of the QWs to relax the strain resulting from the lattice mismatch between the QW structure and the substrate. Next, five CdTe QWs, 117 Å, wide were grown, separated by 300 Å $\text{Cd}_{1-y}\text{Mg}_y\text{Te}$ barrier layers. Magnesium composition y was chosen as high as 33% in order to assure that more than one confined state is present in the QW. Growth of each of the QWs was interrupted for the deposition of a single probe consisting of 2 monolayers of $\text{Cd}_{1-x}\text{Mn}_x\text{Te}$ with intentional Mn molar fraction of 12%. For schematics of the probing heterostructure, see Fig. 1b. Four samples with different positions of the probe layer along the QW axis were grown. Additionally, a reference sample with no probe was prepared.

To obtain exciton transition energies and Zeeman splitting we measured transmission as a function of magnetic field. To optically access the QWs, we first had to remove the nontransparent GaAs substrate, which was done by mechanical polishing and wet etching in hydrogen peroxide. The thick transparent buffer produced Fabry-Pérot oscillations, which obscured the absorption spectrum and thus most of it was removed by chemical etching in a 0.6% solution of bromine in methanol. The sample was immersed in superfluid liquid helium at a temperature of 1.8 K. Magnetic field up to 7 T was applied in Faraday configuration. A halogen lamp was used as a white-light source and the transmission signal was detected by a liquid nitrogen cooled CCD camera and a monochromator. In order to analyze transitions in two circular polarizations, a quarter wave-plate and a linear polarizer were placed in the way of the transmitted beam.

III. RESULTS AND DISCUSSION

Optical density spectra were evaluated according to Beer-Lambert law as $A = -\log(I/I_0)$, where I and I_0 are transmitted and incident beam intensities, respectively. In Fig. 1, we show the spectra obtained from a sample with the probe layer located at the center of the QW. Transitions corresponding to three heavy hole excitons, labelled (n_{el}, n_{hh}) with $n = 1, 2, 3$ numbering electron and heavy hole states, can be resolved. Only diagonal transitions, i.e. those satisfying $n_{el} = n_{hh}$, are observed. The oscillator strength of parity-allowed non-

diagonal transitions is very low, since in a deep rectangular QW the eigenstates are nearly orthogonal. The feature below the (2,2) transition is related to the light hole (1,1) exciton. The increase of the absorption at 2.1 eV is due to $\text{Cd}_{1-y}\text{Mg}_y\text{Te}$ barrier excitons. Immediately from Fig. 1 the effect of the Mn probe layer the exciton Zeeman splitting can be deduced: the odd number excitons exhibit a giant Zeeman effect since there is a non-vanishing PD of finding carriers in the center of the QW (see Fig. 1). On the other hand, the Zeeman splitting of the (2,2) state is limited to the direct interaction between carriers and the magnetic field and so splitting is smaller than the transition line-width.

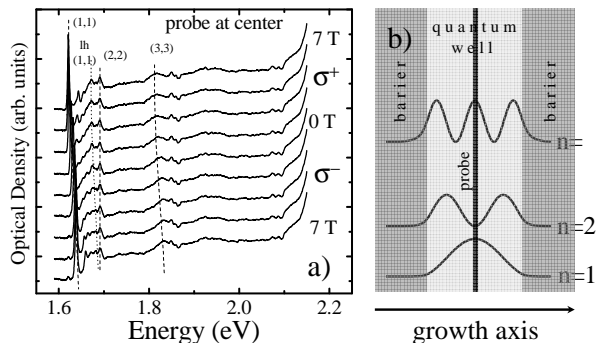


FIG. 1: Left: Optical density spectra for various magnetic fields obtained for a sample with the probe layer at the center of the quantum well. Right: Schematic of this sample shown together with the first three electron PD functions.

The identification of the excitonic transitions in Fig. 1a is based on results of effective mass approximation calculations of electron and hole energy levels in the QW as a function of the magnetic field. In the calculations, we took into account the diffusion of the probe interfaces during growth. The broadened probe shape was modeled by a gaussian function³. The band-edge Zeeman splitting of the probe was described by a modified Brillouin function⁶ with effective parameters S_0 and T_0 reflecting the antiferromagnetic coupling between the Mn ions adjusted to take into account the nonuniform number of nearest neighbors. Valence band states were calculated using a 4x4 Luttinger Hamiltonian¹³. The lattice mismatch between the barrier and the QW layer introduced a strain, which was taken into account in the framework of the Bir-Pikus theory by adding a complete deformation potential Hamiltonian¹⁴. We neglected all the excitonic effects and used the exciton binding energy as a free parameter. In Fig. 2, we present the experimental and calculated transition energies for the same sample as in Fig. 1, i.e. with the Mn probe layer in the center of the QW. Heavy hole exciton binding energies resulting from the presented fits were found to be between 14 and 19 meV remaining in good agreement with calculations in framework of an analytical model by Mathieu *et al.*¹⁵, which yields for (1,1) exciton a binding energy of 14

meV. A very good agreement between the measured and calculated transition energies points out that the model includes the most important features of the system.

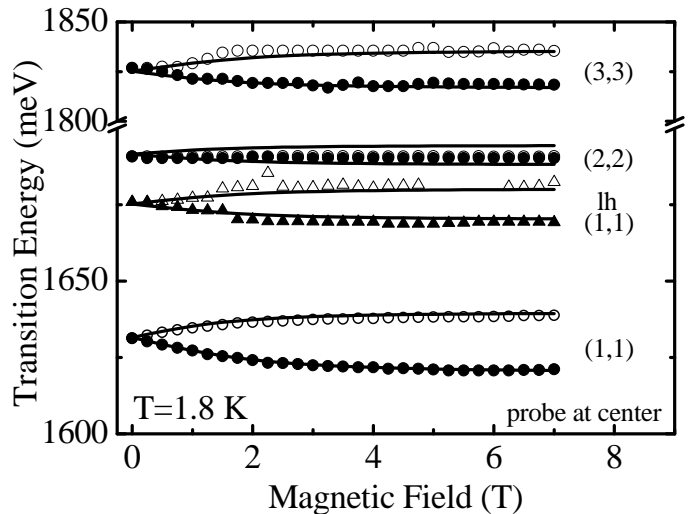


FIG. 2: Points: Exciton transitions measured for a sample with the probe layer at the center of the quantum well. Lines: The results of effective mass calculations allowing the identification of the transitions. Full (empty) points correspond to transitions seen in σ^+ (σ^-) polarization.

Using the above procedure for the reference sample with a flat (i.e. without the probe layer) QW, we fitted the excitonic transitions and calculated electron and heavy hole PD functions $|\varphi_c(z)|^2$ and $|\varphi_v(z)|^2$. In Fig. 3a, we plot these functions weighted with exchange constants as derived in Eq. 5 for the first three QW eigenstates. On the same graph, we present the exciton Zeeman splitting ΔE_Z measured as a function of the position of the center of the probe layer Z_{Mn} . A very good correlation between the Zeeman splitting and the PD value at Z_{Mn} is obtained confirming that the Zeeman splitting provides a good estimation of the PDs. In Fig. 3b, we plot the flat-QW PDs weighted with band offsets as derived in Eq. 7. On the same graph, we plot the exciton energy shifts ΔE_S given by the difference between transition energies for the samples with probe layers and the reference sample with a flat QW. The shifts for the (1,1) and (2,2) excitons are measured and for the remaining (3,3) is calculated since this transition could not be resolved in the reference sample. Again, a good correlation between the measured shift and the PD at the probe location is obtained.

The accuracies of our mapping procedures are summarized in Figs. 3c and d, which show how the measured Zeeman splittings and excitonic shifts are correlated with values of PD functions weighted with exchange integrals and band offsets, respectively. In both cases, we obtain correlation coefficient values $R \approx 0.9$, proving a high accuracy of the approach. Inaccuracies are caused mainly by the fact that the probe layer has a nonzero thick-

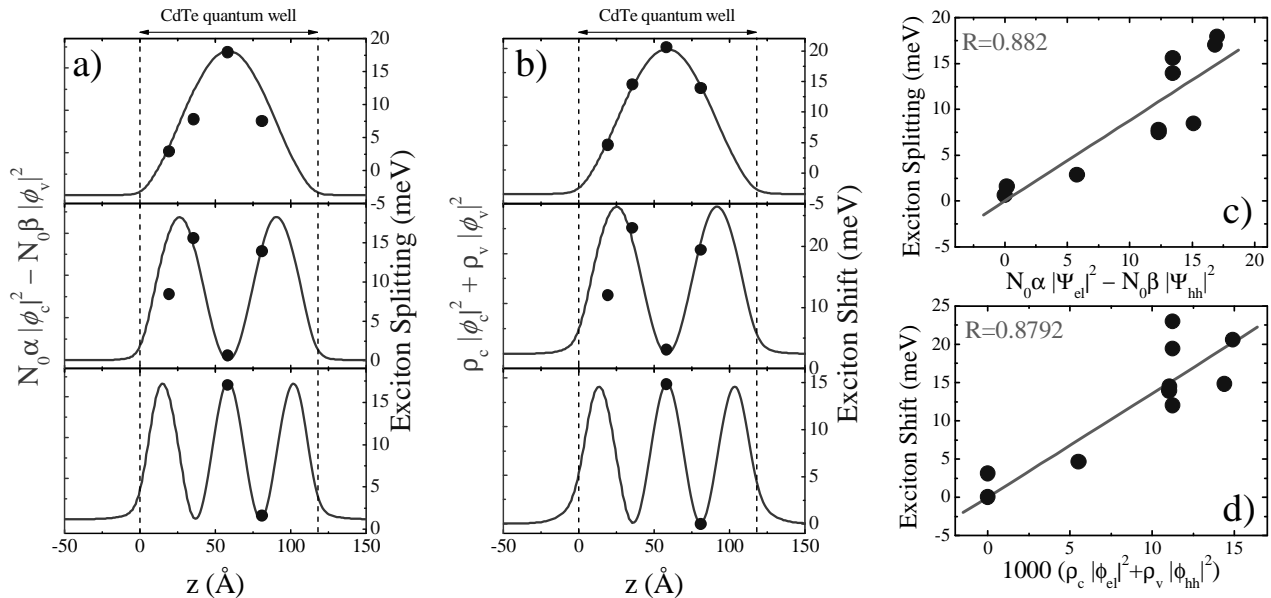


FIG. 3: a) The PD functions of three lowest quantum well eigenstates weighted with exchange constants (lines) and corresponding Zeeman splittings (points, right scale) plotted as a function of the probe layer location. b) The PD functions of three lowest quantum well eigenstates weighted with conduction and valence band offsets (lines) and corresponding exciton shifts (points, right scale) plotted as a function of the probe layer location. c) and d) Correlations between weighted PD functions and Zeeman splitting and exciton shifts, respectively.

ness, contrary to the assumption taken to derive Eqs. 5 and 7. Indeed, two monolayers deposited during growth are further broadened by the intermixing of the interface profile. To fit the excitonic transition dependencies on the magnetic field (see Fig. 2), we had to introduce a gaussian broadened profiles with halfwidths between 2.5 and 4 monolayers depending on the sample. Our effective mass approximation calculations show that this nonzero thickness of the probe layers leads to a noticeable modification of the PD functions. In the PD functions compared with measured quantities in Figs. 3 also not included are the excitonic effects. The electron-hole Coulomb interaction modifies importantly the shape of PD functions with respect to a noninteracting case. A method to obtain Coulomb-correlated φ_c and φ_v is based on a Hartree approach. In this calculation the electron wave function is self-consistently calculated by solving a one dimensional Schrödinger equation with an effective potential resulting from the hole wave function and vice-versa¹⁶. Since in CdTe the hole is about 5 times heavier than the electron, the Coulomb-correlated φ_c tends to unperturbed φ_v . For this reason, previous works on Zeeman mapping successfully compared the results to only heavy hole PD functions^{3,5}.

Another issue not included in the above considerations is the variation of the exchange constants with confinement. As pointed out by Mackh *et al.*¹⁷ and Merkulov *et al.*¹⁸, an admixture of higher \mathbf{k} -vector states leads to a significant decrease of the exchange parameters. Pos-

sible reasons include turning on the kinetic exchange between the conduction electrons and localized Mn ions¹⁸ and a hopping interference in the valence band¹⁷. In our case, both effects would have highest impact on the (3,3) state – the one with highest admixture of the nonzero- \mathbf{k} states¹⁸. We compared the PDs weighted with exchange integrals that were decreased according to the higher- \mathbf{k} states admixture and found a worse agreement with measured Zeeman splittings. We therefore conclude that the reduction of the exchange integrals is less important than the effects related to a nonzero thickness of the probe layers.

In order to obtain a higher mapping accuracy one should design thinner (e.g. submonolayer) mapping probes that introduce a smaller perturbation potential. In that case, the observed Zeeman splitting and the shift of the excitonic transition will be smaller, but one will gain a weaker modification of the mapped PD functions. Another approach is to completely bury the semimagnetic probes in a CdMgTe QW exploiting the same band offsets for MgTe and MnTe with respect to CdTe^{10,19}. In this method, the Mn composition of the probes and the Mg composition of the QW bottom are chosen to assure a flat QW potential so at zero magnetic field no perturbation is introduced. Applying a small magnetic field should make mapping feasible with only a minor modification of the PD functions.

In summary, we have compared two independent methods for mapping of the quantum well eigenstates with

semimagnetic probes. One is based on the analysis of the position of exciton transition which in the first order of perturbation theory is proportional to a value of a wave function weighted with band offsets. The second approach exploits the fact that for samples with thin semimagnetic probes the exciton Zeeman splitting is pro-

portional to a value of a wave function weighted with exchange constants. We find a good agreement between the calculated wave functions and measured excitonic positions and Zeeman splittings and we conclude that both methods are equally well suited for mapping purposes.

-
- ¹ J.-Y. Marzin and J.-M. Gérard, Phys. Rev. Lett. **62**, 2172 (1989).
- ² G. Salis, B. Graf, K. Ensslin, K. Campman, K. Maranowski, and A. C. Gossard, Phys. Rev. Lett. **79**, 5106 (1997).
- ³ G. Prechtel, W. Heiss, A. Bonnani, W. Jantsch, S. Maćkowski, E. Janik, and G. Karczewski, Phys. Rev. **B 61**, 15617 (2000).
- ⁴ G. Yang, J. K. Furdyna, and H. Luo, Phys. Rev. **B 62**, 4226 (2000).
- ⁵ S. Lee, M. Dobrowolska, J. K. Furdyna, and L. R. Ram-Mohan, Phys. Rev. **B 59**, 10302 (1999).
- ⁶ J. K. Furdyna, J. Appl. Phys. **64**, R29 (1988).
- ⁷ A. Mauger and D. L. Mills, Phys. Rev. **B 31**, 8024 (1985).
- ⁸ G. Prechtel, W. Heiss, A. Bonnani, W. Jantsch, S. Maćkowski, and E. Janik, Phys. Rev. **B 68**, 165313 (2003).
- ⁹ J. A. Gaj, G. Planel, and R. Fishman, Solid State Comm. **29**, 435 (1979).
- ¹⁰ M. Kutrowski, T. Wojtowicz, G. Cywinski, G. Karczewski, E. Janik, E. Dynowska, J. Kossut, P. Kossacki, R. Fiederling, A. Pfeuffer-Jeschke, et al., Acta Phys. Pol. **A 92**, 887 (1997).
- ¹¹ J. Sivianiant, F. V. Kyrychenko, Y. G. Semenov, D. Coquillat, D. Scalbert, and J. P. Lascaray, Phys. Rev. **B 59**, 10276 (1999).
- ¹² W. Grieshaber, A. Haury, J. Cibert, Y. M. d'Aubigné, A. Wasiela, and J. A. Gaj, Phys. Rev. **B 53**, 4891 (1996).
- ¹³ J. M. Luttinger, Phys. Rev. **102**, 1030 (1956).
- ¹⁴ G. L. Bir and G. E. Pikus, *Symmetry and Strain-induced Effects in Semiconductors* (Wiley, New York, 1974).
- ¹⁵ H. Mathieu, P. Lefebvre, and P. Christol, Phys. Rev. **B 46**, 4092 (1992).
- ¹⁶ F. V. Kyrychenko, S. M. Ryabchenko, and Y. G. Semenov, Physica E **8**, 275 (2000).
- ¹⁷ G. Mackh, W. Ossau, A. Waag, and G. Landwehr, Phys. Rev. **B 54**, 5227 (1996).
- ¹⁸ I. A. Merkulov, D. R. Yakovlev, A. Keller, W. Ossau, J. Geurts, A. Waag, G. Landwehr, G. Karczewski, T. Wojtowicz, and J. Kossut, Phys. Rev. Lett. **83**, 1431 (1999).
- ¹⁹ B. Kuhn-Heinrich, W. Ossau, H. Heinke, F. Fischer, T. Litz, A. Waag, and G. Landwehr, App. Phys. Lett. **63**, 2932 (1993).